Electronic Supplementary Information for

Phosphatidyl-assisted fabrication of graphene oxide nanosheets with multi-active sites for uranium(VI) capture

Peipei Yang[a,d], Qi Liu[a,d], Hongsen Zhang[a,e], Jingyuan Liu[a,d], Rongrong Chen[a,d], Rumin Li[a,c,d], Di Wu[b], Xuefeng Bai[d] and Jun Wang[a,c,d*]*

[a.] Key Laboratory of Superlight Material and Surface Technology, Ministry of Education, Harbin Engineering University, 150001, P. R. China.

[b.] Institute of Theoretical Chemistry, Jilin University, Changchun 130023, P. R. China.

[c.] Harbin Engineering University Capital Management Co. Ltd., P. R. China

[d.] College of Material Science and Chemical Engineering, Harbin Engineering University, 150001, P. R. China

[e.] Modern Analysis, Test and Research Center, Heilongjiang University of Science and Technology, Harbin 150027, P. R. China.

Corresponding author: Email: zhqw1888@sohu.com, qiliu@hrbeu.edu.cn

SI.1 Adsorption studies.

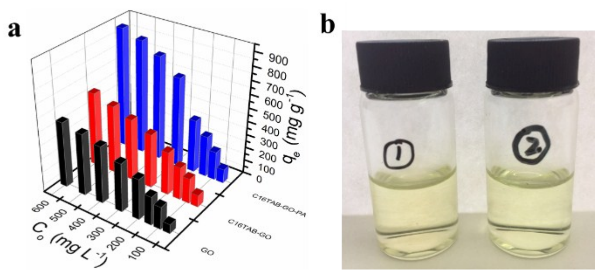

Figure S1. Effect of concentration of U(VI) adsorption onto GO, GO-C_{16}TAB and GO-C_{16}TAB-PA composites (a) and the digital photos for pH=8 of uranium(VI) solution (b) (C_o=525.5 mg L^{-1} (1) and 623.3 mg L^{-1} (2))

SI.2 Kinetics study

As the sorption kinetics govern the residence time of the sorption reaction and determine the solute uptake rate or the efficiency of the reaction, the following pseudo-first-order, pseudo-second-order and Weber-Morris (W-M) models are employed to interpret the mechanism controlling the sorption process. The linear form of the two models can be expressed by the following Eqs. S1-S3:

$$\ln\left(q_e - q_t\right) = lnq_e - k_1 t \qquad \text{(S1)}$$

$$t/q_t = 1/k_2 q_e^2 + t/q_e \qquad (S2)$$

$$q_e = K_{ip}\sqrt{t} + C \qquad \text{(S3)}$$

Where q_t and q_e (mg g^{-1}) are the capacity of U(VI) at time t (min) and at equilibrium, K_{ip} is Internal diffusion constant, respectively, and k_1 (min^{-1}) and k_2 (g mg^{-1} min^{-1}) are the respective rate constants.

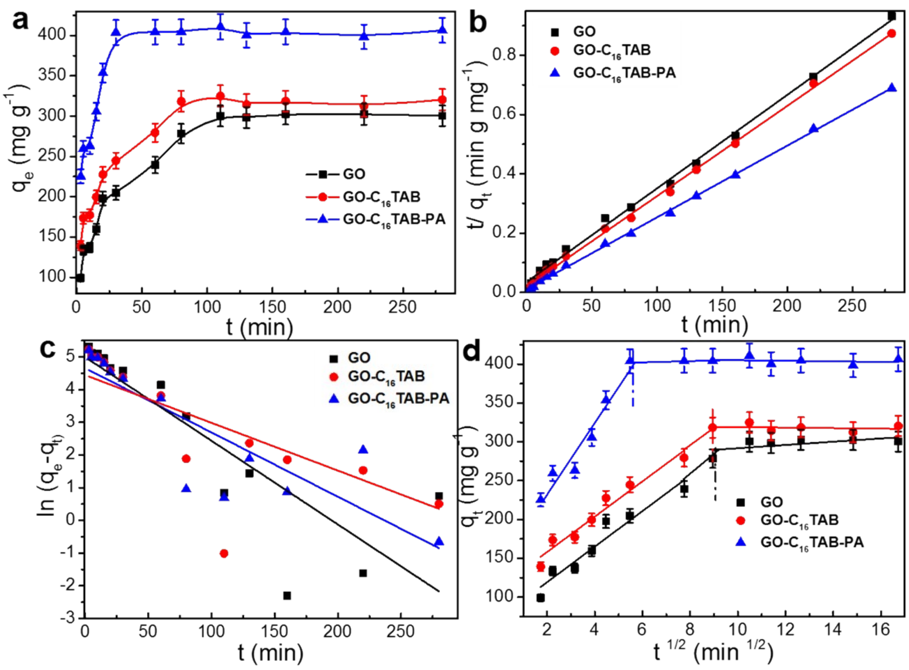

Figure S2. Effect of a) contact time, b) pseudo-second-order, c) pseudo-first-order, and d) Weber–Morris order plot, for the removal of U (VI) onto GO, GO-C_{16}TAB and GO-C_{16}TAB-PA composites, pH= 8.00; T= 25 ^oC; amount of adsorbent 0.01 g and C_o=200 mg L^{-1}.

Table S1 Kinetic parameter for adsorption of U (VI)

Kinetics model	U(VI) initial concentration	Materials	K	q_e^{exp}	q_e^{cal}	R^2
Pseudo-first order	200 mg g^{-1}	GO	0.0256	279	85	0.71044
		GO-C_{16}TAB	0.0146	319	105	0.70211
		GO-C_{16}TAB-PA	0.01966	407	148	0.72048
Pseudo-first order	500 mg g^{-1}	GO	0.0167	476	294	0.80274
		GO-C_{16}TAB	0.0121	540	138	0.70633
		GO-C_{16}TAB-PA	0.0234	981	137	0.92426
Pseudo-second order	200 mg g^{-1}	GO	$2.7*10^6$	279	317	0.99917
		GO-C_{16}TAB	$5.1*10^6$	319	327	0.99854
		GO-C_{16}TAB-PA	$8.6*10^6$	407	413	0.99753
Pseudo-second order	500 mg g^{-1}	GO	$2.2*10^7$	476	495	0.99918
		GO-C_{16}TAB	$1.6*10^8$	540	552	0.99935
		GO-C_{16}TAB-PA	$1.0*10^9$	981	1004	0.99975

SI.3 Isotherms study

In order to probe the maximum adsorption capacity and the progress of adsorption, the adsorption isotherms was studied. The adsorption of U (VI) on the GO, GO-C_{16}TAB and GO-C_{16}TAB-PA composites increased with increasing temperature and the Langmuir and Freundlich models were applied to simulate experimental data.

$$C_e/q_e = 1/b \cdot q_m + C_e/q_m \qquad \text{(S4)}$$

$$\ln q_e = \ln k + 1/n ln C_e \qquad \text{(S5)}$$

$$\ln q_e = ln\, q_m - \beta\varepsilon^2 \qquad \text{(S6)}$$

Where q_e (mg g^{-1}) is the amount of U (VI) adsorbed at adsorbent capacity at equilibrium, β is activity and ε is the Polanyi potential. In this formula, ε was calculated by the following equations:

$$\varepsilon = RTln\,(1 + {}^{1}/{C_e}) \quad \text{(S7)}$$

$$E = 1/\sqrt{2\beta} \quad \text{(S8)}$$

Where C_e (mg L^{-1}) is the equilibrated U (VI) concentration, q_e (mg g^{-1}) is the amount of U (VI) adsorbed on the adsorbents capacity at equilibrium. K (L mg^{-1}) is a Langmuir constant related to the energy of the adsorbent and q_m (mg g^{-1}) is the saturation capacity at complete monolayer coverage.

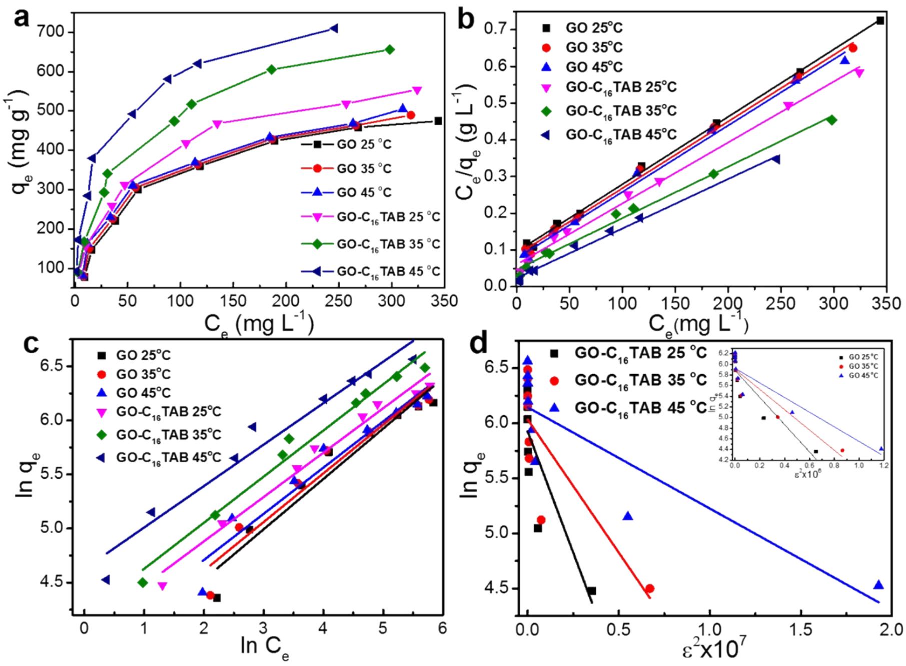

Figure S3. a) Isotherm model for GO-C_{16}TAB-PA composites; b) Langmuir model; c) Freundlich model; d) Dubinin-Radushkevich model of GO-C_{16}TAB-PA.

Table S2 Isotherm parameter for adsorption of U (VI)

Materials	T (K)	Langmuir isotherm				Freundlich isotherm		
		q^{exp} (mg g^{-1})	q_o (mg g^{-1})	b (L mg^{-1})	R^2	K (L mg^{-1})	n	R^2
GO	298	474.6	534	0.1823	0.99887	36.23	2.14	0.92893
	308	489.4	549	0.2769	0.99839	40.86	2.22	0.93282
	318	505	552	0.3635	0.99271	47.20	2.34	0.92684
GO-C_{16}TAB	298	554.6	602	0.2034	0.99858	57.59	2.34	0.94869
	308	656.4	714	0.2897	0.99769	66.72	2.43	0.96533
	318	710	741	0.3142	0.99391	102.17	2.61	0.9769
GO-C_{16}TAB-PA	298	875.4	1014	0.2489	0.99842	180.80	1.71	0.83439
	308	930.5	1111	0.3664	0.99912	291.51	2.14	0.87132
	318	953.1	1182	0.3678	0.99958	487.77	2.64	0.88349

Table S3. The values of E for GO, GO-C_{16}TAB and GO-C_{16}TAB-PA

Material	E (KJ mol^{-1})		
	298.15 K	308.15 K	318.15 K
GO	7.91	8.03	8.81
GO-C_{16}TAB	8.52	9.21	10.02
GO-C_{16}TAB-PA	9.32	10.32	11.68

In order to calculate a series of thermodynamic parameters of the adsorbent, and this subsequent chemical equation is utilized.

$$\ln K_d = \frac{\Delta S^\circ}{R} - \frac{\Delta H^\circ}{RT} \tag{S9}$$

$$\Delta G^o = \Delta H^o - T\Delta S^o \tag{S10}$$

$$K_d = \frac{q_e}{C_e} = \frac{(C_o - C_e)}{C_e} \cdot \frac{V}{m} \tag{S11}$$

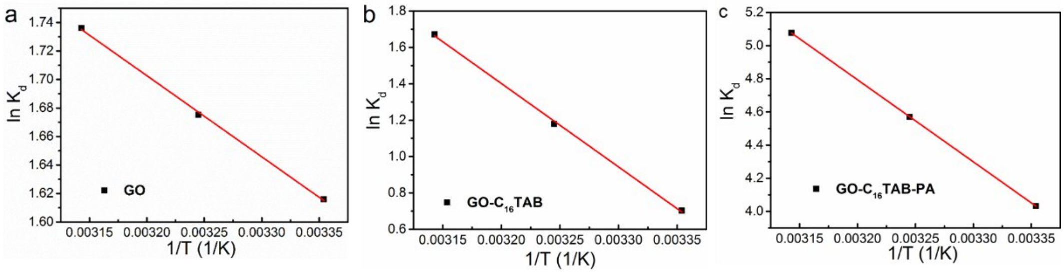

Figure S4. The influence of temperature on the U(VI) sorption on the GO (a), GO-C_{16}TAB (b) and GO-C_{16}TAB-PA (c) relationship curve between ln K_d and 1/T (1/K). pH= 8.0; T= 25 ^oC; amount of adsorbent 0.01 g and t= 230 min.

Table S4 The thermodynamic parameters of GO, GO-C_{16}TAB and GO-C_{16}TAB-PA for U(VI) adsorption

material	ΔH^o (kJ mol^{-1})	ΔS^o (J mol^{-1} K^{-1})	ΔG^o (kJ mol^{-1})		
			298.15K	308.15K	318.15K
GO	21.13	29.29	-8.71	-9.04	-9.29
GO-C_{16}TAB	38.16	133.75	-39.84	-41.18	-42.51
GO-C_{16}TAB-PA	41.15	171.54	-51.1	-52.82	-54.53

SI.4 Effect of co-existing ions on GO, GO-C_{16}TAB and GO-C_{16}TAB-PA adsorbents

The selectivity coefficient (S_U) for U(VI), is defined as a specific term to describe the potency and degree of selectivity of the adsorbents as follows:

$$S_U = \frac{K_d^U}{K_d^M} \qquad \text{(S9)}$$

Where K_d^U and K_d^M are the distribution ratio of the U(VI) ion and other competing ions in sorbent and solution, respectively.

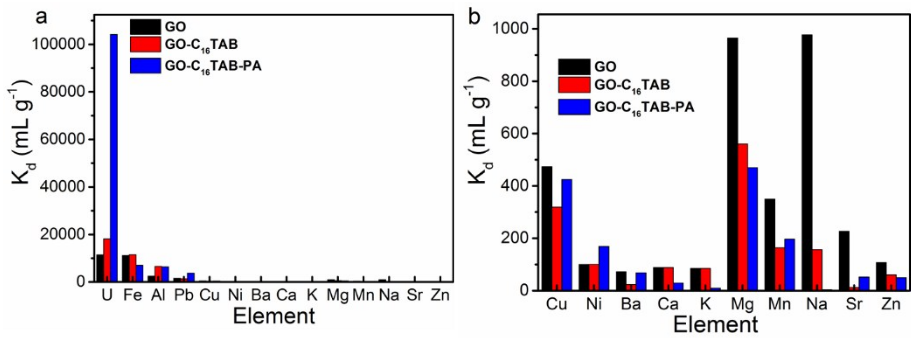

Figure S5. The K_d value of co-existing ions on the removal of U(VI) by GO, GO-C_{16}TAB and GO-C_{16}TAB-PA composites.

Table S5 The selectivity coefficients ($S_{U/M}$) of U(VI) for different metal ions in water.

	Fe	Al	Pb	Cu	Ni	Ba
GO $S_{U/M}$	1.03	4.61	7.23	24.19	114.37	159.15
GO-C_{16}TAB $S_{U/M}$	1.58	2.77	13.31	56.86	181.36	775.21
GO-C_{16}TAB-PA $S_{U/M}$	14.89	16.34	27.95	245.07	617.93	1538.06

	Ca	K	Mg	Mn	Na	Sr	Zn
GO $S_{U/M}$	130.29	134.87	11.86	32.79	11.72	50.51	107.05
GO-C_{16}TAB $S_{U/M}$	206.59	213.87	32.37	110.72	115.6	1473.22	302.2
GO-C_{16}TAB-PA $S_{U/M}$	3581.22	11460.74	221.73	530.69	27132.9	1994.25	2100.81

SI.5 Adsorption-desorption experiments

SI.5.1 U (VI) desorption experiments

The recyclability and reuse of adsorbents play an important role in the extraction of U(VI) from seawater. The eluent agents of NaCl, citric acid, HNO_3, $NaHCO_3$, and NaOH were first investigated for desorption of U(VI). The results from Table S6 demonstrate that HNO_3 is the best eluent agent for reuse and recyclability of GO, GO-C_{16}TAB and GO-C_{16}TAB-PA adsorbents. In the typical experiment, 20 mg of sorbent with U(VI) ions was added into 50 mL eluent solution, which included in 0.1 mol L^{-1} NaCl, 0.1 mol L^{-1} Citric acid, 0.1 mol L^{-1} HNO_3, 0.1 mol L^{-1} $NaHCO_3$ and 0.1 mol L^{-1} NaOH, respectively. The flasks were stirred for specified time (t, min) at room temperature, and then the solid phase was separated from the solution by centrifuge. The results were analysed with WGJ-III Trace Uranium Analyser to obtain the concentrations of U (VI) ions. The elution rate of U (VI) ions was calculated.

Table S6 The elution efficiency of different eluents

Eluent	Elution efficiency (%)		
	GO	GO-C_{16}TAB	GO-C_{16}TAB-PA
0.1 mol L^{-1} NaCl	38.6	35.8	33.5
0.1 mol L^{-1} Citric acid	52.4	45.6	43.6
0.1 mol L^{-1} HNO_3	88.5	89.3	90.3
0.1 mol L^{-1} $NaHCO_3$	37.3	30.9	25.1
0.1 mol L^{-1} NaOH	45.2	55.2	60.6

In regard to the above findings, we examined the effect of different concentrations of HNO_3 for adsorption-desorption of U(VI) onto GO, GO-C_{16}TAB and GO-C_{16}TAB-PA. The results were given in Table S7, indicate that the change in eluent rate responds smoothly to increasing concentration of HNO_3, especially when nitrate concentrations are above 0.1 mol L^{-1}. Taking into account these factors and cost issues, 0.1 mol L^{-1} HNO_3 was used for the next step, which is the regeneration of GO, GO-C_{16}TAB and GO-C_{16}TAB-PA adsorbents for U(VI).

Table S7 The elution efficiency of different concentrations of HNO_3.

Concentration (mol L^{-1})	Elution efficiency (%)		
	GO	GO-C_{16}TAB	GO-C_{16}TAB-PA
0.02	69.8	67.3	65.8
0.04	75.3	72	73
0.06	80	81.4	80.6
0.08	84.8	83.7	85.2
0.1	88.5	89.3	90.3
0.2	90.5	90.8	91.3
0.4	90.9	90.5	91.4
0.6	90.8	91.1	91.3
0.8	91.2	91.3	91.8

SI.5.2 U (VI) absorption-desorption cycle experiments

In a typical experiment, 20 mg of sorbent was added into 50 mL of U (VI) solution and stirred for 6 h at room temperature. The solid phase was separated from the solution by centrifuge. Then, the adsorbent in the vacuum drying oven for 24 h. The dried sorbent was placed in the 50 mL eluent solution (0.1 mol L^{-1} HNO_3) for the 6 h. After elution, the GO, GO-C_{16}TAB and GO-C_{16}TAB-PA composites was washed with abundant deionized water to remove residual H^+ and UO_2^{2+} until cannot detect UO_2^{2+} in the aqueous solutions. The GO, GO-C_{16}TAB and GO-C_{16}TAB-PA composites were regenerated by drying at 80 °C for 24 h and then reused. Eventually the elution efficiency of U (VI) ions was calculated. Repeat this experiment operation for six times.

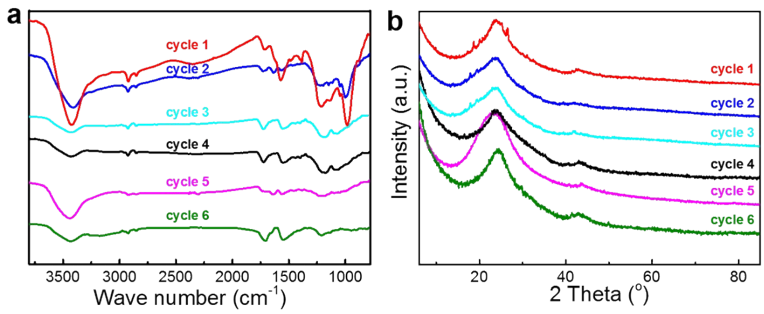

Figure S6. The FTIR spectra and XRD of GO-C_{16}TAB-PA composites after 6 cycles.

SI.6 Mechanism of adsorption

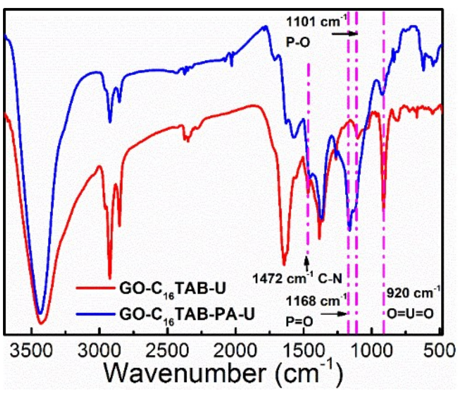

Figure S7. FTIR of after and before for U(VI) onto the GO-C_{16}TAB and GO-C_{16}TAB-PA composites.

Table S8 Comparison of sorbent performance of GO-composites with literature data

Adsorbents	q_m (mg g^{-1})	pH	Contact time (min)	Ref.
Ethylenediaminetetraacetic acid-graphene oxide	213	6	180	1
Phosphate-functionalized graphene oxide	252	4	240	2
Sulfonated graphene oxide	310	6	80	3
Halloysite@graphene oxide	161	7	240	4
Amino functionalized magnetic graphene oxide	141	6	100	5
Nickel ferrite /graphene oxide	135	5	180	6
Graphene oxide/ polydopamine	145	4	180	7
Magnetic cucurbit[6]uril/graphene oxide	123	5	150	8
GO-C_{16}TAB-PA	923	8	60	Present study

1. S. Liu, H. Zhang, D. Peng, D. Yuan, L. Wu and J. Ma, Uranium uptake with graphene oxide sponge prepared by facile EDTA‐assisted hydrothermal process, *Internat. J. Energ. Res.*, 2017, **41**, 263-273.
2. X. Liu, J. Li, X. Wang, C. Chen and X. Wang, High performance of phosphate-functionalized graphene oxide for the selective adsorption of U(VI) from acidic solution, *J. Nucl. Mater.*, 2015, **466**, 56-64.
3. Z. B. Zhang, Y. F. Qiu, Y. Dai, P. F. Wang, B. Gao, Z. M. Dong, X. H. Cao, Y. H. Liu and Z. G. Le, Synthesis and application of sulfonated graphene oxide for the adsorption of uranium(VI) from aqueous solutions, *J. Radioanal. Nucl. Ch.*, 2016, **310**, 1-11.
4. J. Xiao, S. Xie, Y. Jing, Y. Yao, X. Wang and Y. Jia, Preparation of halloysite@graphene oxide composite and its application for high-efficient decontamination of U(VI) from aqueous solution, *J. Mol. Liq.*, 2016, **220**, 304-310.
5. L. Chen, D. Zhao, S. Chen, X. Wang and C. Chen, One-step fabrication of amino functionalized magnetic graphene oxide composite for uranium(VI) removal, *J. Colloid Interf. Sci.*, 2016, **472**, 99-107.
6. L. P. Lingamdinne, Y. L. Choi, I. S. Kim, J. K. Yang, J. R. Koduru and Y. Y. Chang, Preparation and

characterization of porous reduced graphene oxide based inverse spinel nickel ferrite nanocomposite for adsorption removal of radionuclides, *J. Hazard. Mater.*, 2017, **326**, 145-156.

7. Z. Zhao, J. Li, T. Wen, C. Shen, X. Wang and A. Xu, Surface functionalization graphene oxide by polydopamine for high affinity of radionuclides, *Colloid. Surface. A*, 2015, **482**, 258-266.
8. L. Shao, X. Wang, Y. Ren, S. Wang, J. Zhong, M. Chu, H. Tang, L. Luo and D. Xie, Facile fabrication of magnetic cucurbit[6]uril/graphene oxide composite and application for uranium removal, *Chem. Eng. J.*, 2016, **286**, 311-319.